

## Supporting Information

### Nanocube $\text{In}_2\text{O}_3$ @RGO heterostructure based gas sensor for acetone and formaldehyde detection

Rajneesh Kumar Mishra,<sup>a§</sup> G. Murali,<sup>a</sup> Tae-Hyung Kim,<sup>b</sup> Jee Hun Kim,<sup>b</sup> Young Jin Lim,<sup>a</sup> Byoung-Suhk Kim,<sup>c</sup> P. P. Sahay<sup>d</sup> and Seung Hee Lee<sup>\*a</sup>

<sup>a</sup>Applied Materials Institute for BIN Convergence, Department of BIN Fusion Technology and Department of Polymer-Nano Science and Technology, Chonbuk National University, Jeonju, Jeonbuk 561-756, Korea.

<sup>b</sup>Graduate School of Flexible & Printable Electronics Engineering, Chonbuk National University, Jeonju, Jeonbuk 561-756, Korea.

<sup>c</sup>Department of Organic Materials & Fiber Engineering and Department of BIN Fusion Technology, Chonbuk National University, Jeonju, Jeonbuk 561-756, Korea.

<sup>d</sup>Department of Physics, Motilal Nehru National Institute of Technology Allahabad, Allahabad-211004, India.

\*Correspondence to Prof. Seung Hee Lee, [ls1@chonbuk.ac.kr](mailto:ls1@chonbuk.ac.kr), Tel: +82-63-270-2343

---

§ Current Affiliation: Department of Electronic Engineering, Incheon National University, Incheon, 406-772, Korea.

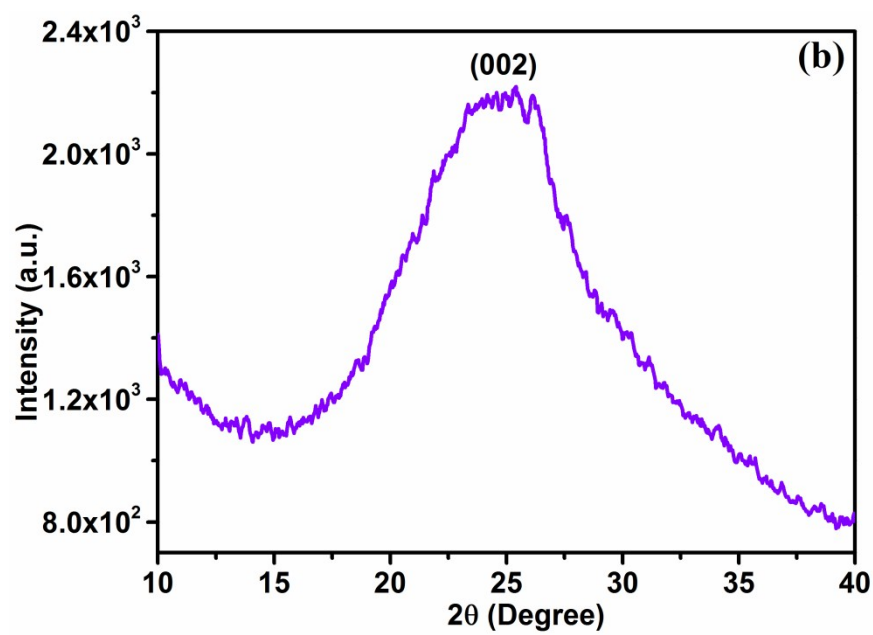
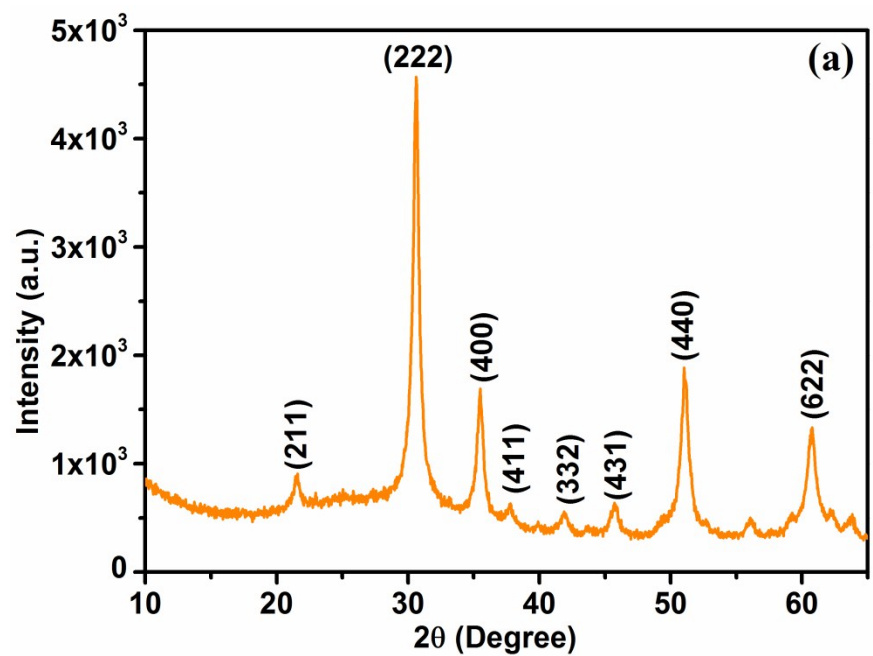


Fig. S1: XRD spectra of the as synthesized  $\text{In}_2\text{O}_3$  nanocubes (a) and RGO (b).

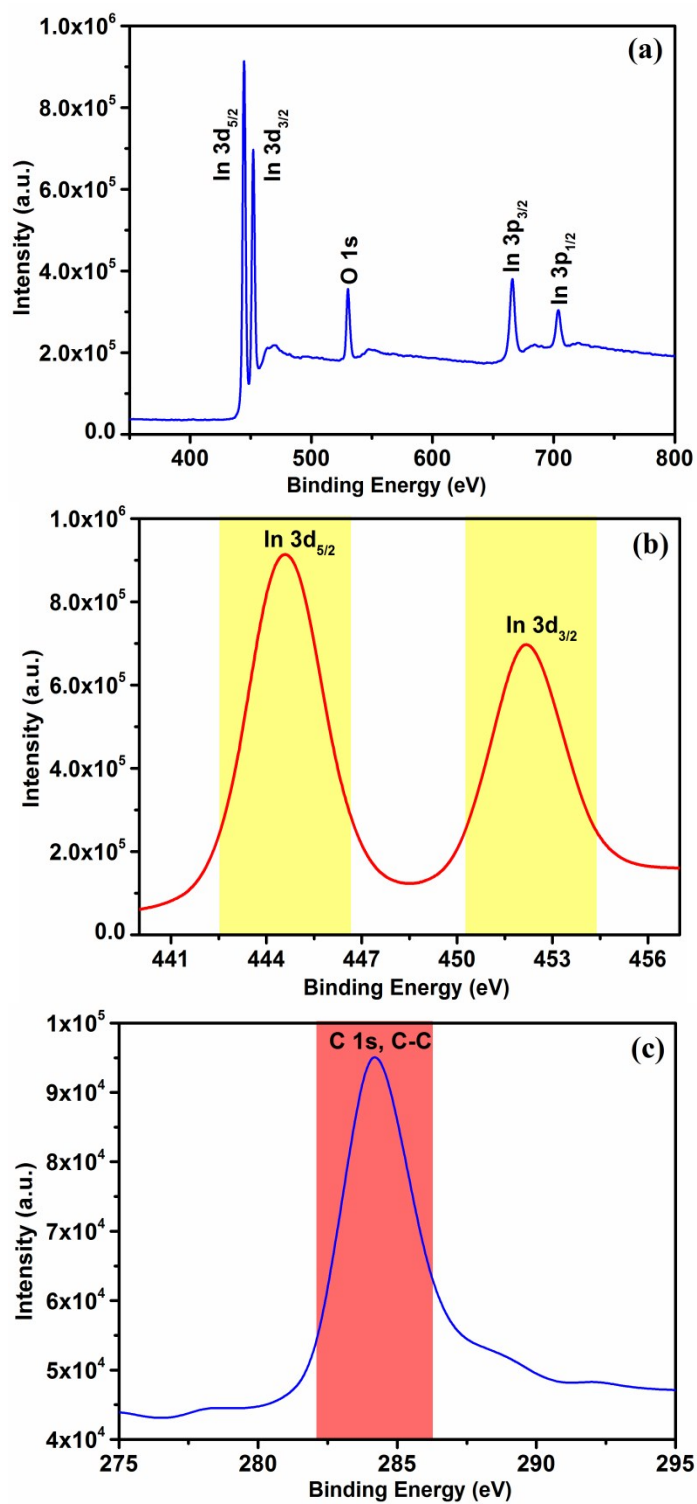
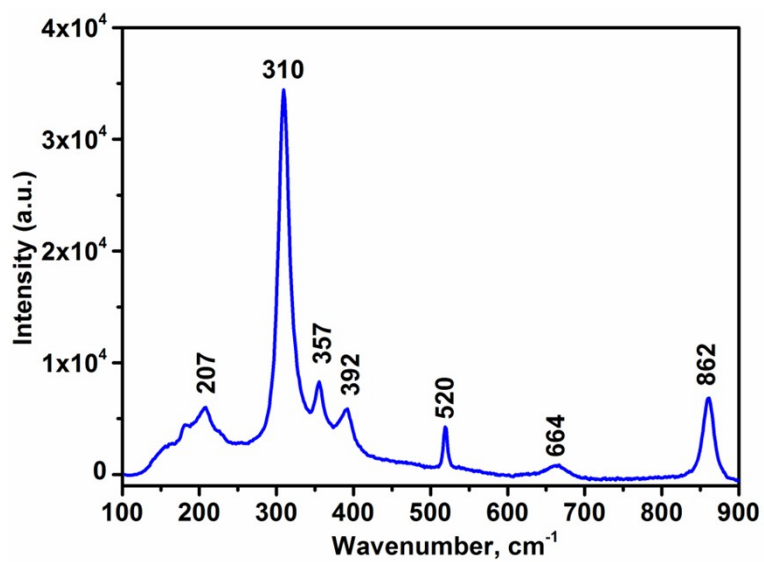
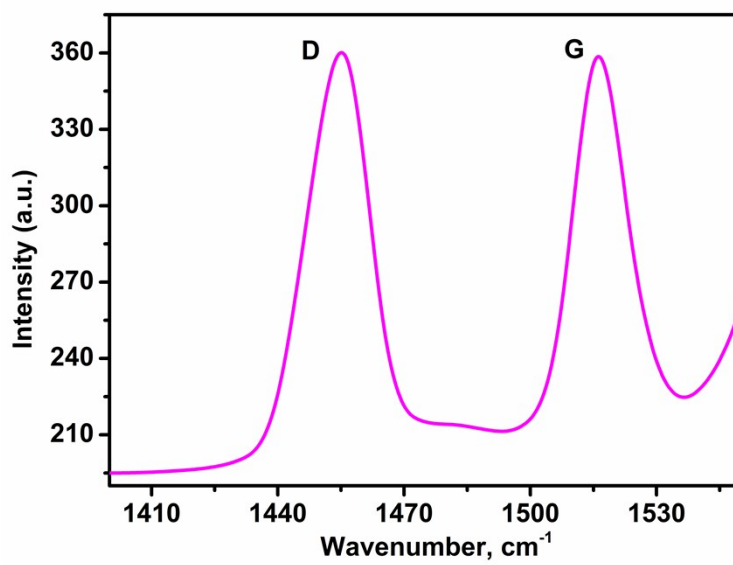


Fig. S2: XPS survey spectra of In<sub>2</sub>O<sub>3</sub> nanocube (a), deconvoluted spectrum of In 3d peaks (b) and RGO C 1s peak (c).

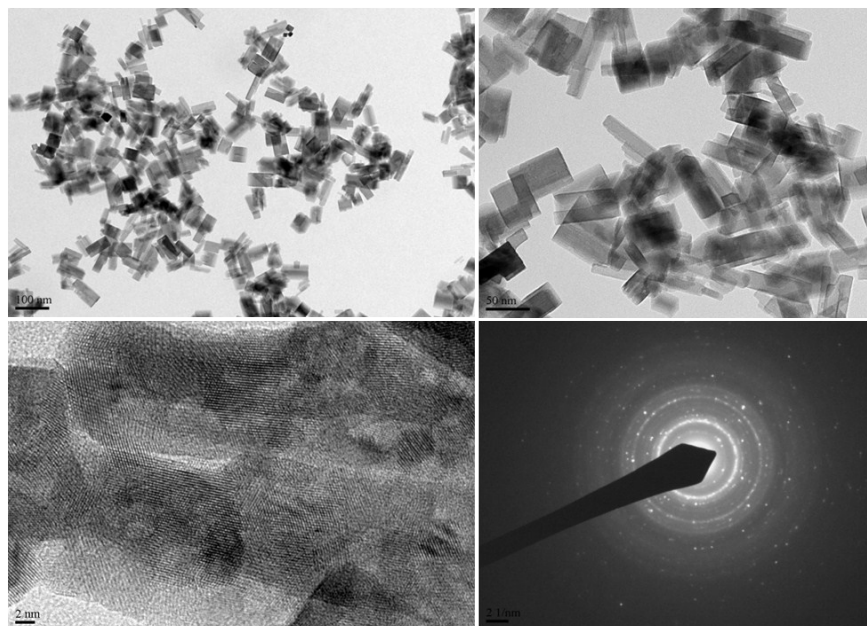


(a)

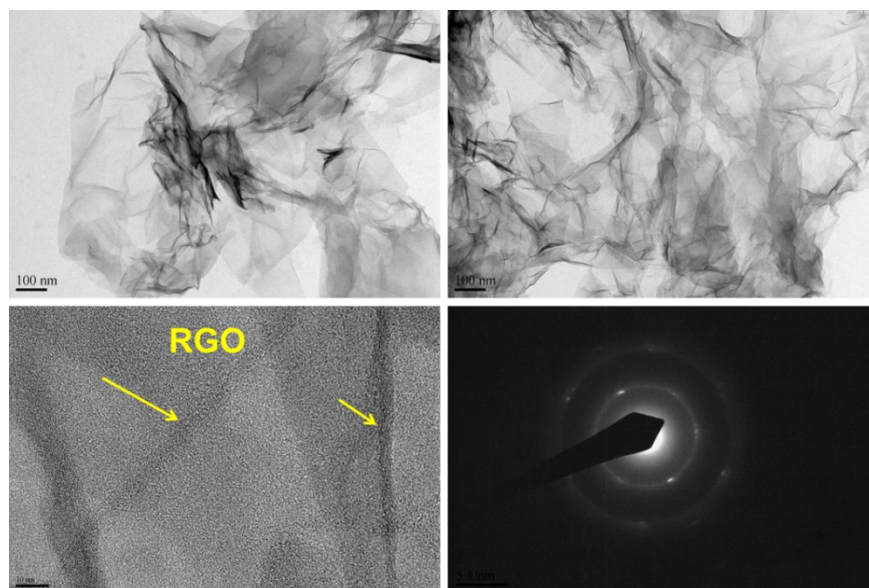


(b)

Fig. S3: Raman spectrum of the  $\text{In}_2\text{O}_3$  nanocube (a) and RGO (b).

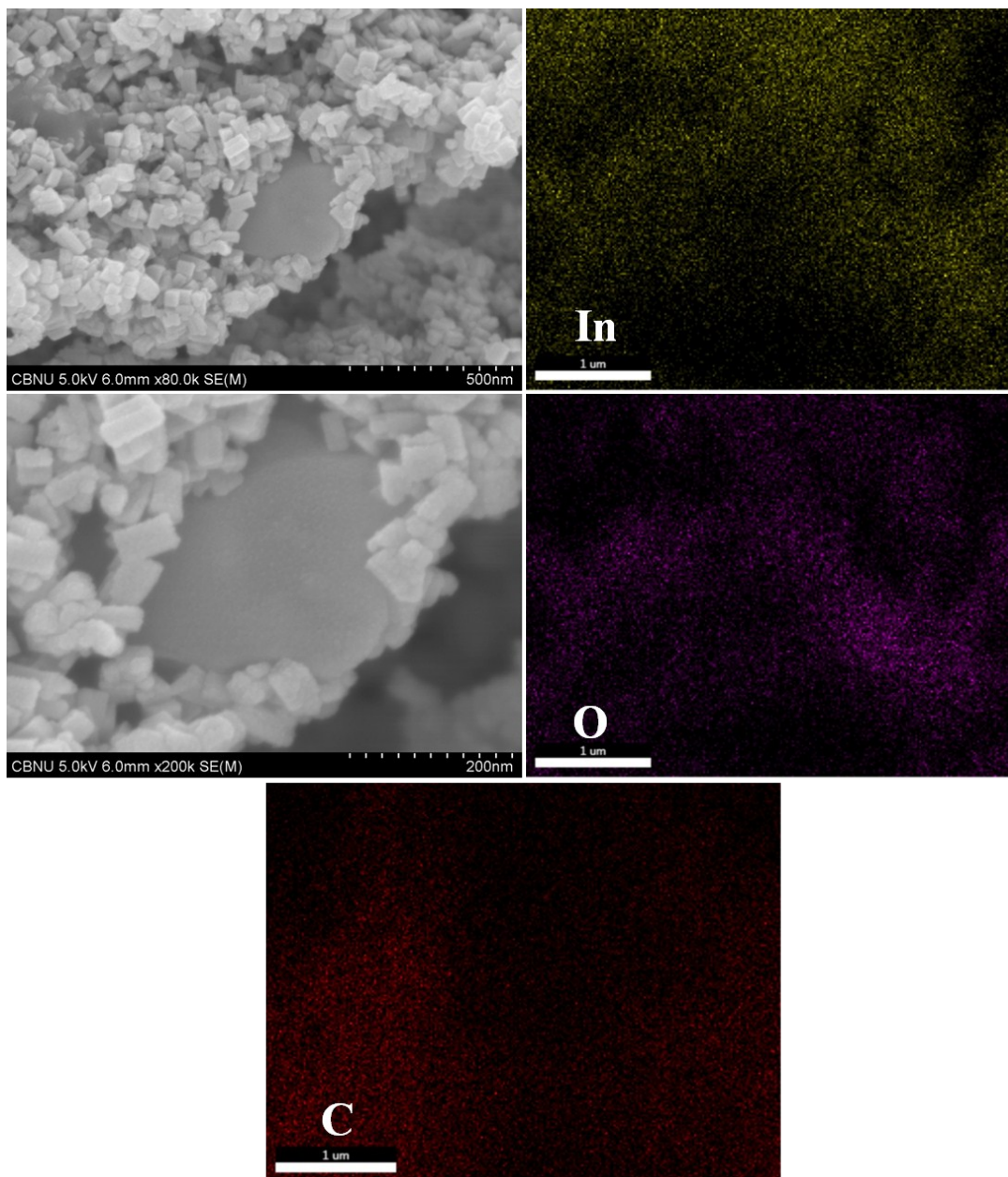


(a)

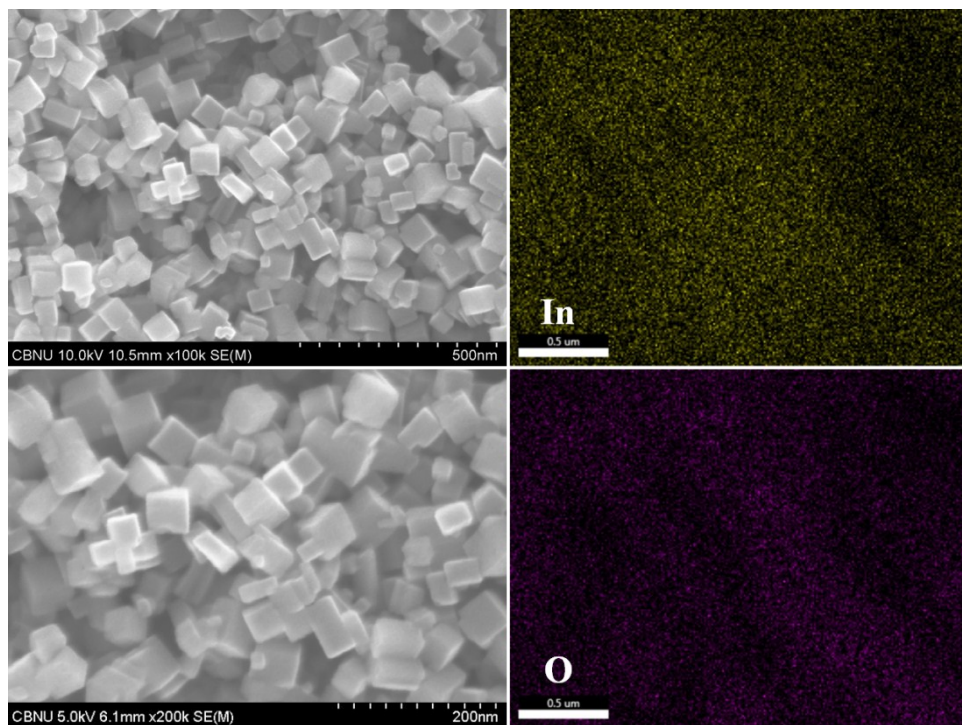


(b)

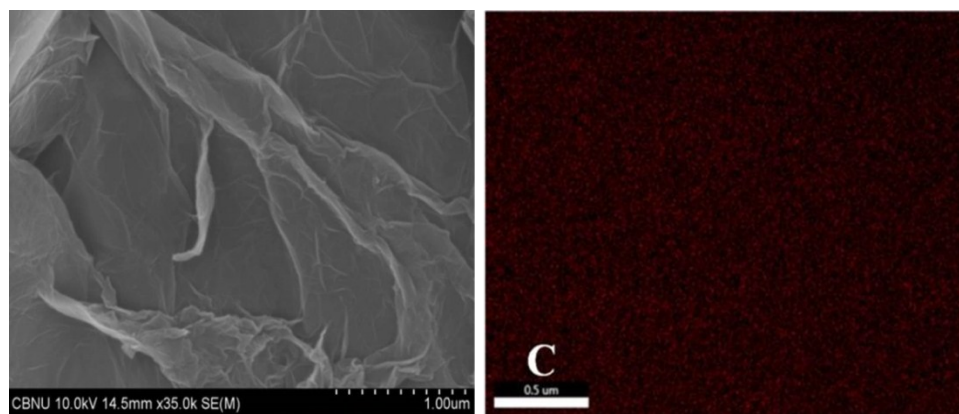
Fig. S4: The TEM, HR-TEM images and SAED pattern of the as synthesized (a)  $\text{In}_2\text{O}_3$  nanocube and (b) RGO.



(a)



(b)



(c)

Fig. S5: FE-SEM images and corresponding elemental mapping of the as synthesized nanocube  $\text{In}_2\text{O}_3$ @RGO heterostructure (a),  $\text{In}_2\text{O}_3$  nanocube (b) and RGO (c).

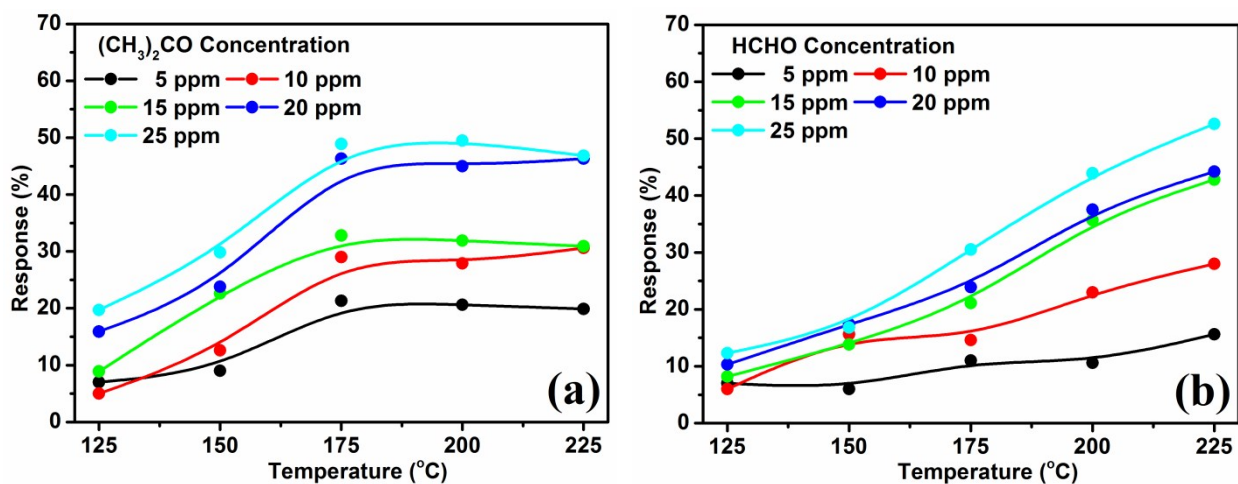


Fig. S6: Acetone (a) and formaldehyde (b) gas sensing characteristics of the  $\text{In}_2\text{O}_3$  nanocube sensor as a function of operating temperature for various concentrations.

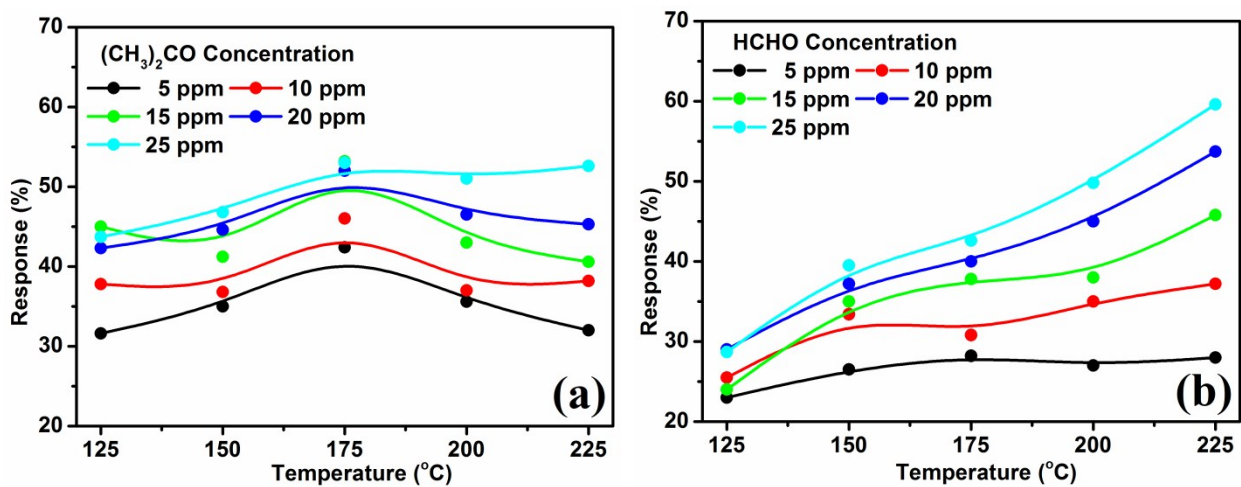


Fig. S7: Acetone (a) and formaldehyde (b) gas sensing characteristics of the RGO sensor as a function of operating temperature for various concentrations.

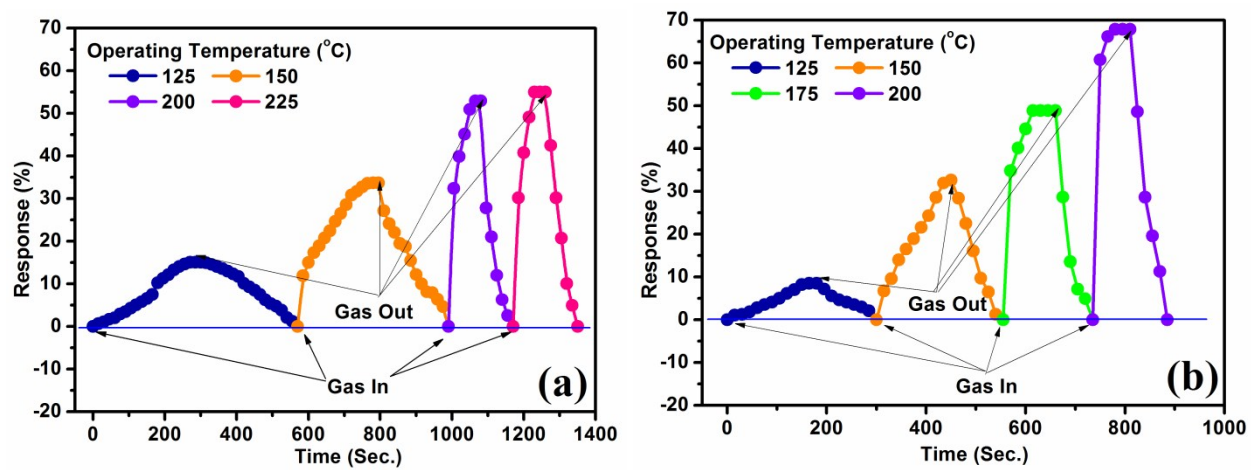


Fig. S8: Acetone (a) and formaldehyde (b) transient response characteristics of the nanocube  $\text{In}_2\text{O}_3@\text{RGO}$  heterostructure sensor at different operating temperatures for 25 ppm concentration.